Available online at www.sciencedirect.com

ScienceDirect

Procedia Structural Integrity 24 (2019) 225–232

Structural Integrity Procedia

www.elsevier.com/locate/procedia

AIAS 2019 International Conference on Stress Analysis

Numerical investigation of wire-clamp contact for a drawing machine

Chiara Colombo[a]*, Andrea Ceresetti[b], Stefano Dall'Acqua[b], Laura Vergani[a]

[a] *Politecnico di Milano, Department of Mechanical Engineering, via La Masa 1, 20156 Milano, Italy*
[b] *Marcegaglia Specialties, via A.I.D.O. 3, 46049 Contino di Volta Mantovana (MN), Italy*

Abstract

Machines for cold wire drawing are widely spread in the industrial field to reduce wires' section. The system is complex, because the axial pulling force has to correctly deform wires into the drawing dies. The present work focuses on a continuous press and pulling system, with a track-chain. Normal force at the steel clamps can be generated independently on the axial force, but avoiding slipping and local yielding at the external surface of the wire. The work presents a numerical model of wire-clamp contact, focusing on the yielded area at the wire surface, and aimed at the identification of the limit clamping force that avoids slipping and yielding. Reliability of results is critically discussed, based on the choice of element formulation and type, and mesh refinement. Based on this analysis, control parameters of the drawing machine are modified to experimentally verify this limit normal force estimated by the numerical model.

Keywords: Contact mechanics; wire drawing machine; numerical analysis.

1. Introduction

Machines for continuous cold wire drawing are widely spread in industrial field to obtain rods or wires of reduced sections for a wide range of applications, e.g. automotive, electrical and civil engineering, etc. The core of this process is the reduction of the wire cross section by pulling it into one or more conical dies, with the aim of improving the

* Corresponding author. Tel.: +39-02-2399-8667; fax: +39-02-2399-8263.
E-mail address: chiara.colombo@polimi.it

10.1016/j.prostr.2020.02.019

mechanical strength. Drawing machines are quite complex systems, because the axial pulling force has to correctly deform the wires into the drawing dies according with analytical equations, as underlined in the past by Wistreich (1958) and Yang (1961). This literature has focused mainly on the deformation in the dies, influenced by many factors, such as wire chemistry, approach angle, lubrication, drawing speed and lubricant, reduction ratio, die wear, etc. Recent literature, Sas-Boca et al (2017) and Kyo Kabayama et al. (2009), is also interested in the development of numerical tools, based on die geometry, able to estimate wire deformation and to optimize and control the process, save energy and limit wear on the dies. Some numerical studies also dealt with multi step drawing, including thermomechanical calculations, such as Celentano et al (2009), Celentano (2010) and Filice et al. (2013). These studies underline that, despite wire drawing is a well-known process, there is still an industrial interest, supported by academic research, in the optimization of the setup and process parameters.

The present work focuses on the pulling system of a cold wire drawing machine, installed in an industrial plant. The pulling machine applies the axial force to the wire by a mechanical track, connected with a series of steel clamps. By means of a control system, clamps press and pull the wire with a continuous operation. The machine design allows to generate the normal force at the clamps independently on the axial force, but within certain limitations. More in details, given the axial force to deform the wire into the dies, the corresponding normal force at the clamps must avoid: 1) slipping and 2) local yielding of the wire surface. This last point is particularly critical for the wire object of this study, because, if the surfaces of the wires are damaged, the following treatment of plating could be compromised.

The aim of this study is to select suitable working parameters to avoid local plastic deformation, i.e. yielding, at the surface of the wires, considered as a damage, in correspondence of the clamp contacts. This study is carried out by means of a non-linear numerical approach based on finite elements (FE) and on the concepts of contact mechanics, Wriggers (2006).

Before we started this numerical analysis, the pulling machine was governed in displacement control. During this study, the setup of the pulling system of the drawing machine was changed, allowing for a force control. Therefore, results of the numerical model will focus on the applied contact force, normal to the clamp, as a percentage of the axial force required to pull the wire and to guarantee the needed plastic deformation in the dies.

2. Framework of the wire drawing machine

All the wires produced with the original configuration of the pulling machine experienced surface damages with plasticized regions, periodically reproduced and clearly related to the pulling system. Four strips of plasticized regions could be observed, corresponding to the four contact points at the claps of the pulling system. There was no evidence of misalignment of the wire with respect to the drawing direction, therefore the attention was focused on the clamping of the pulling system. Moreover, it was noted that these damages were more visible when the clamps were newly regenerated, while they were less marked when the clamps were worn; this suggested that the problem was the clamping.

These surface marks are particularly critical for the wire object of this study, because it has to withstand plating and has to ensure final aesthetic requirements. These regions at the wire surface, plastically deformed, will result in periodic irregularities not acceptable for the final product from the aesthetic viewpoint. Before this study, the industrial practice was to produce it by an old-generation cam-to-cam machine; this operation is affected by low productivity compared to actual standard and the industry is interested in avoiding it, focusing on a better control of the drawing track-chain machine; and in particular optimizing the ratio between the normal and axial forces applied at the clamps.

3. Experimental measure of the damage

In order to experimentally quantify the damage occurring to the wire, an optical 3D surface measurement system was used, Alicona InfiniteFocus. This is a non-contact tool that automatically generates a high-resolution image of the surface, allowing for a specific measurement of surface shape and roughness. We scanned an area 80 mm long and 2 mm wide, around the damaged region. The measure was repeated for the 4 strips of some wires, i.e. 360° rotation with respect to the wire axis.

Fig.1 shows a cross section of the damaged region, in correspondence of the highest damage. The profile underlines a non-constant depth of the plasticized region. At the beginning of the plastic strip the depth is around 7μm, then it

increases to 15μm (maximum measured value) after 10mm along the wire axis, i.e. the drawing direction, and decreases to 6μm from the central area to the end. The measure of the width is less simple, due to the wire curvature. In general, it is observed that in the regions where the depth is higher, the width is smaller, and vice versa. Moreover, there is no evidence of slipping, especially at the beginning of the strip, when the contact starts at the clamp chamfer.

This experimental damage measure suggests that this surface damage depends on the contact force imposed to the camping system during the pulling operation, thus the machine requires a better control to work in an optimal configuration.

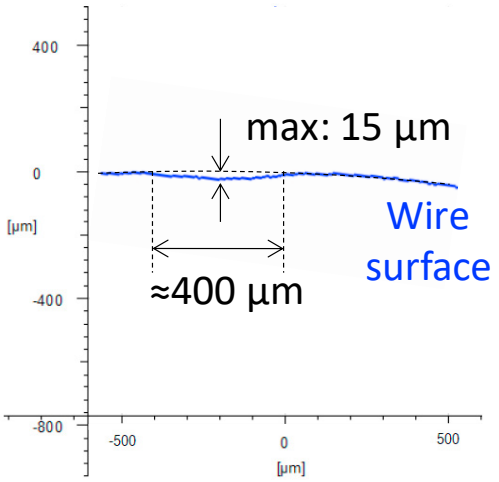

Fig.1. Experimental measure of the damaged profile of the wire surface.

4. The numerical model

The numerical model is implemented with the FE software Abaqus by Simulia. We hypothesized that all the clamps pushing the wire surface undergo the same maximum force normal with respect to the bar surface, i.e. there is no fluctuation or overloads of the normal force while the wire passes through the considered machine. For this reason, we modelled only one clamp, and not all the clamps simultaneously pressing and pulling the wire.

The assembly is composed of two parts: the steel clamp and a segment of the wire. For symmetry reasons, we considered only half of the clamp and one quarter of the wire (see Fig.2.a). The clamps have a V-shape with a characteristic angle: this allows to use the same clamp for wires of different diameters.

Since we are interested in stresses and strains occurring at the wire surface, we considered the semi-clamp as an infinitely rigid body, i.e. made of 4-node 3D bilinear rigid quadrilateral (according with Abaqus nomenclature: R3D4, see Simulia (2017)). This choice is conservative with respect to the stress state at the wire surface, that we are investigating. A reference point is placed at the center of the upper face of the schematized clamp (Fig.2.b). Boundary conditions are applied to the symmetry surface and to this reference point, to constrain the clamp to the only movement along y direction. Indeed, we initially simulated also the rotation, based on a kinematic analysis of the drawing machine, but no contact occurs during the rotation. In other words, the damage occurs when the clamp is parallel to the wire.

The reference point of the semi-clamp is pushed towards the wire with force control.

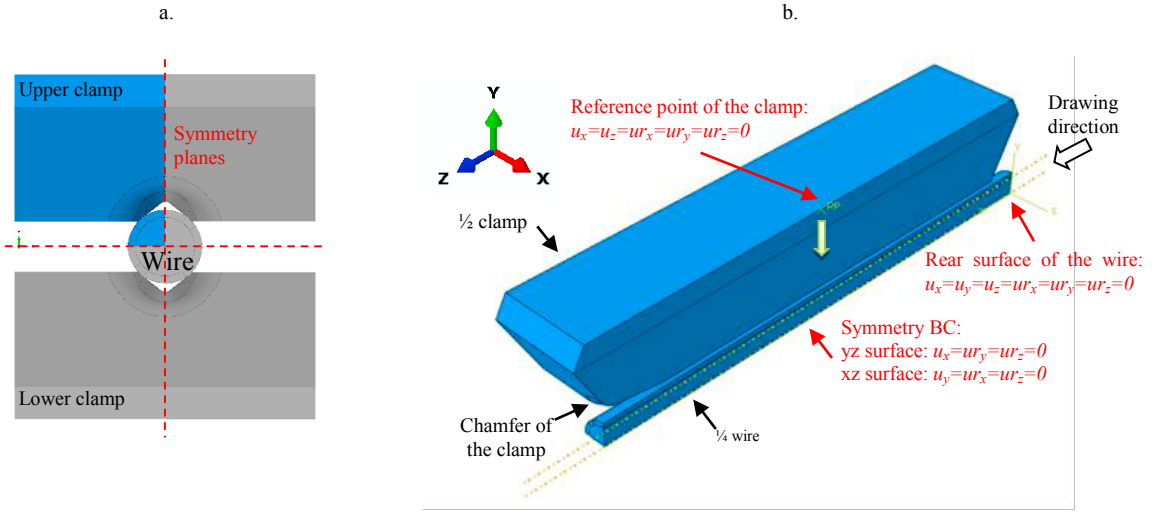

Fig.2. Geometry of the model: (a) *xy* plane with identification of symmetry planes and effective schematized geometry in blue; (b) assembly with boundary conditions of the problem. *u* are the displacements and *ur* are the rotations. *z* axis is the drawing direction of the wire.

The wire is a rod with 10 mm diameter, made of S235JRC steel. Experimental static tensile tests were performed to obtain the mechanical characteristics: yielding stress $R_{p0.2}$ = 534 MPa, ultimate tensile strength UTS = 562 MPa, and elastic modulus E = 200 GPa; Poisson ratio is set to 0.3. We considered a bilinear stress-strain curve for the numerical model.

Abaqus considers different deformable elements' types and formulations, having pros and cons for the contact problem faced in this work. According with Abaqus nomenclature, the available continuum 3D finite elements with hexahedral shape and linear shape functions are (Fig.3):

1) C3D8, bricks with 8 nodes placed at each corner and 8 integration points (full integration), see Fig.3.a;
2) C3D8R, with reduced integration, i.e. with a unique integration point at the centroid, see Fig.3.b. They are the simplest and allow reducing computational time and output size, even if they are the less accurate;

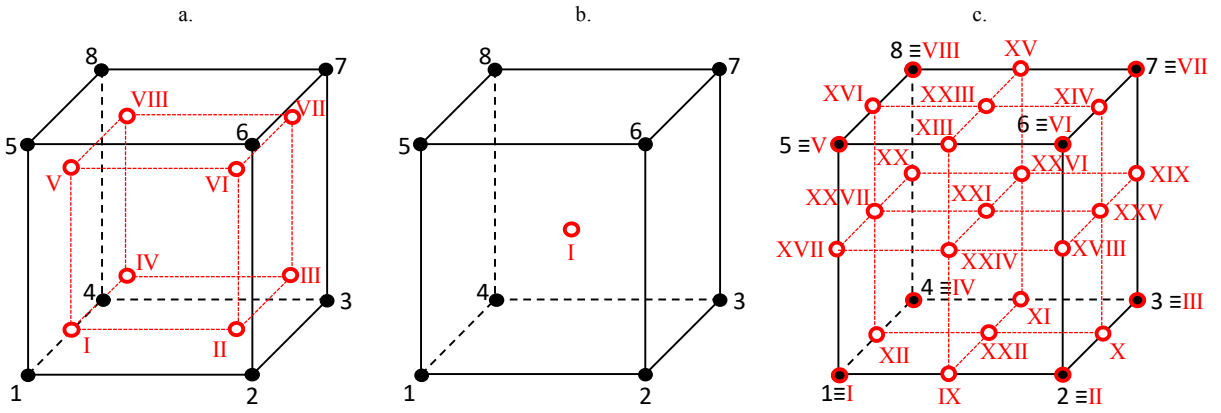

Fig.3. Types of continuum 3D finite elements with hexahedral shape and linear shape functions, used for the wire:
(a) C3D8, full integration; (b) C3D8R, reduced integration; (c) C3D8S, improved surface stress visualization, according with the commercial nomenclature by Abaqus. Nodes are the black arabic numerals; integration points are the red roman numerals.

3) C3D8S, with improved surface stress visualization. These elements have 27 integration points, see Fig.3.c: 8 are placed at its nodes (corners), 12 at the middle of each edge, 1 at the centroid and 6 at the center of each face. This feature allows these elements to directly estimate field quantities, as stresses and strains, without extrapolating them. In particular, the stresses at the contact surface are not obtained by extrapolation, avoiding errors and obtaining more accurate values. For this reason, these elements are really a good choice for contact mechanics and estimation of stresses at the contact surface. Of course, given their complexity in the numerical formulation, they will require higher computational time and will result in larger output files.

Mesh size for the semi-clamp is 1 mm, with some refinement to 0.5 mm at the chamfer. On the other hand, the choice of element size for the wire is particularly challenging, because of the reduced width of the damage. We performed a convergence study, selecting different mesh sizes at the surface of the wire, i.e. at the contact region, imposing a fixed displacement at the reference point of the clamp and monitoring the resulting normal force (Fig.4.b). Coarse meshes give low or even no details on the damaged region. The selected element size for the wire is 0.1 mm (Fig.4.a).

The contact formulation is set from the beginning of the simulation, i.e. at the initial step. The normal contact behavior is *hard* contact type, using the classical Lagrange multiplier method of constraint enforcement. The friction formulation is penalty (stiffness-based) type with friction coefficient 0.2. This value is hypothesized, and not experimentally measured. The literature reports studies estimating the friction coefficient between 0.08-0.15 for lubricated drawing machines, underlying that it is inversely proportional to the drawing speed (Wistreich (1958), and Kyo Kabayama et al. (2009)). The clamping and pulling system we are analyzing is placed after the dies, and the wire is quite cleaned from the lubricant, therefore we hypothesized a friction coefficient slightly higher with respect to those works.

a. b.

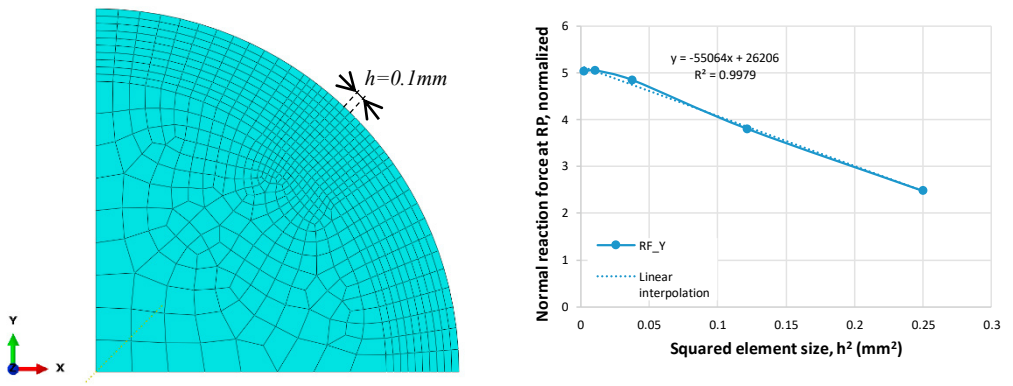

Fig.4. (a) Mesh of the cross section of the wire; *h* identifies the element size at the contact region. (b) convergence study. Values of the normal force at the clamp are normalized with respect to the slip limit force.

5. Selection of the maximum normal force to avoid damage

5.1. Numerical results

The output of the numerical models is analyzed in terms of: 1) contact area, which is a direct output of the simulation, and 2) yielded area, i.e. damaged at the wire surface, which is estimated by summing the areas of the yielded elements at the contact region. Fig.5 shows the trends of the contact and yielded areas as a function of the resulting vertical force at the semi-clamp. This force has been normalized with respect to the slip limit force.

In these plots we added a vertical line corresponding to the slipping limit between the wire and the clamping system.

a. b.

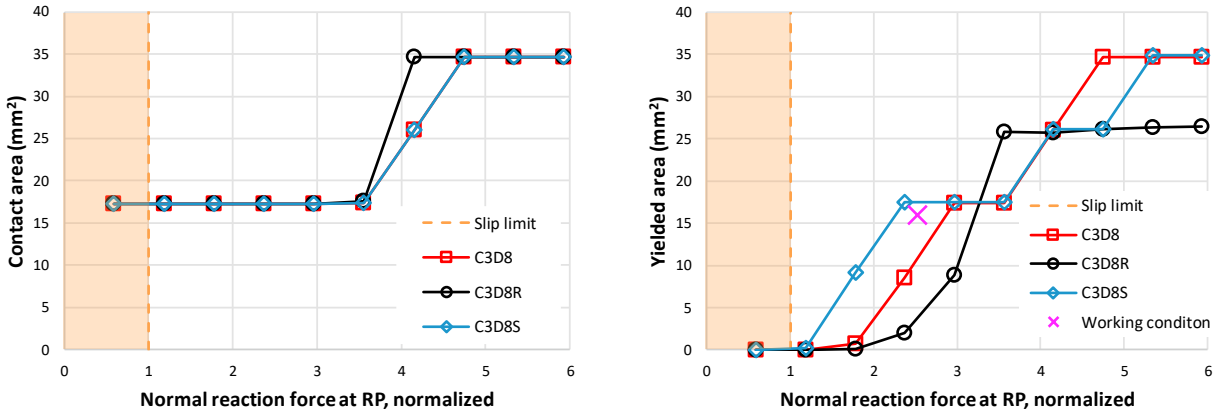

Fig.5. Plots of: (a) contact area; (b) yielded (damaged) area, at the contact region between the semi-clamp and the wire. Areas are function of the normal reaction force, estimated with the FE model at the reference point of the semi-clamp and normalized with respect to the slip limit force.

This limit is analytically computed trough Coulomb's law, based on the imposed axial force, not object of modification, on the given friction coefficient and on the geometry of the clamp, i.e. the angle defining the V-shape. It is not possible to select a pressing force to the camping and pulling system lower than this limit (orange area in the plots); indeed, slippage is a very dangerous working condition for the drawing machine, that will stop of the production.

The contact area of Fig.5.a shows an initial constant value around 17mm^2, which depends on the mesh discretization and local contact shape of the elements. The plot shows the estimation of the contact area by three finite elements. They give very similar information.

On the other hand, Fig.5.b shows the yielded area, where plastic strain occurs at the integration points of the elements. The three curves are shifted progressively to the right if the plot. This behavior depends on the used element type: C3D8R elements have their unique integration point farther from the surface with respect to C3D8 and C3D8S elements, thus they give the less conservative estimation of the yielded area and of the damage occurring at the surface. C3D8 elements have an intermediate behavior, while C3D8S give the most precise information about the surface strain. Indeed, in correspondence of the initial working condition, identified in the plot with the purple cross and based on the experimental measurements described in Sect.3, damage at the surface clearly occurs; therefore, the estimation by C3D8R elements is not acceptable, while C3D8S elements result the most appropriate to estimate this experimental damage. This can be considered a validation of the numerical model with C3D8S elements.

The plot of Fig.5.b is useful also to estimate an optimal working condition for the clamping and pulling system. Indeed, we can propose to decrease the clamping force to at least 2 times the slip limit force. With this force, the C3D8 model does not estimate any plasticized region, while the C3D8S shows limited damage. We preferred not to consider lower clamping forces because the slip limit is function of the friction coefficient, which has not been experimentally measured.

5.2. Analytical calculations

Further estimations of this normal force at the clamps can be performed analytically by the Hertzian contact theory, Hertz (1881). According with this well-known theory, the state of stress at the surface of two contacting cylinders is:

$$\sigma_1 = 0.5 p_H \,, \quad \sigma_2 = \sigma_3 = p_H \,, \quad \tau_{12} = 0 \tag{1}$$

where 1 and 2 are the in-plane direction at the surface, 3 is the axis pointing from the surface to the center of the cylinder, and p_H is the maximum contact (Hertzian) pressure, estimated as:

$$p_H = \frac{2F_N/b}{\pi e} \tag{2}$$

In this last equation, we have that F_N is the normal force pushing the two cylinders, b is the length of the contact region, that can be experimentally measured or numerically estimated, and e is the semi-length of the indentation. Considering that the clamp is flat at the contact region, the expression of e is:

$$e = \sqrt{\frac{4F_N(K_{c1}+K_{c2})\rho_{c2}}{b}} \tag{3}$$

where the under scripts *c1* and *c2* stand for the two contact cylinders, and K are the material ratios:

$$K = \frac{1-\nu^2}{\pi E} \tag{4}$$

Knowing the state of stress at the surface form Eq. (1), we can apply a static criterion for assessment, such as von Mises, to estimate the maximum normal force F_N before yielding. Considering a steel-steel contact, we can estimate a force corresponding to the yielding limit equal to 2.58 the slip limit force. This force is too high, because we experimentally observed the surface damage. On the other hand, considering an infinitely rigid clamp, i.e. $K_{c1} = 0$, the estimated yielding force is equal to 1.36 the slip limit force. This second value of force is nearer to the numerical estimation of 2 times the slip limit force, even if it is quite low and could result in wire slipping. The numerical estimation seems the best solution, because it accounts for the real contact geometry and friction.

5.3. Definition of the allowable working parameters

Finally, we can express the selected normal force as a ratio with respect to the axial force applied to the wire during the drawing operations. Fig.6 shows a plot with the normalized axial and vertical (clamping) forces acting on the simulated system. Both slip and yield limits are given, evidencing areas where the drawing machine is not working in the best conditions. The only region where to select optimal working parameters is the central white triangle. At the beginning of this work, the machine was working with a ratio between normal and axial force equal to 16.0; based on the developed numerical model, we proposed to decrease the normal force, keeping fixed the axial force, thus with a new ratio of 12.6.

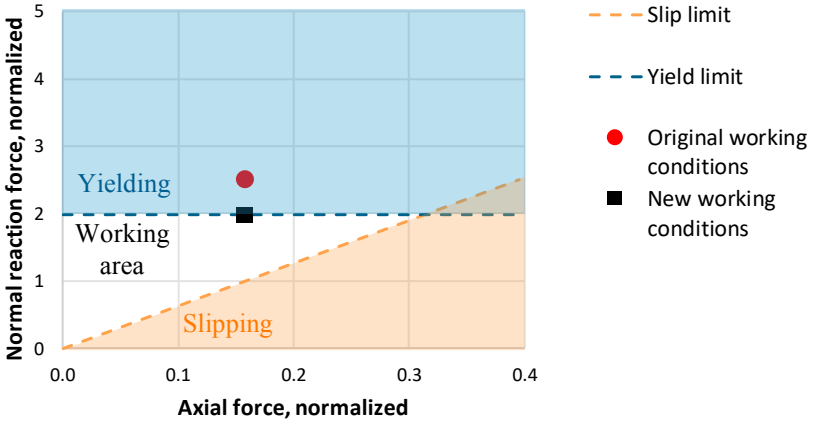

Fig.6. Graphical determination of the optimal working area of the semi-clamp and wire system, considering the axial force pulling the wire and the normal force applied by the semi-clamp.

This plot is not only useful for this specific case, but it supports the operator in the selection of the best parameters of this machine, to avoid slipping and yielding of the wires. Indeed, this numerical model could be a useful predictive tool, because, by simply changing the size of the wire, it could offer good predictions and provide the operator with information about the optimal use of the drawing machine.

It should be mentioned that we performed a trial, decreasing progressively the normal force at the clamps up to the ratio between normal and axial forces equal to 12.6, as from the numerical estimation. When the pulling machine started working at the steady state with these new parameters selected by means of the implemented numerical approach, absence of yielding at the wire surface was eventually verified. This can be considered a further verification of the numerical prediction, thus underlying the practical application of the FE model in this industrial manufacturing context.

6. Conclusions

The work described a numerical approach to solve a practical industrial problem, due to the non-optimal selection of working parameters for the pulling system of a drawing machine. The damage, induced by the original configuration of the machine, is a surface plastic deformation due to the excessive normal force applied at the clamps. From the obtained numerical results, we can draw the following conclusions:

- different FE formulations were implemented to estimate the contact force, having integration points placed at different depths;
- depth and width of the damage were experimentally measured and used to validate the model with integration points at the surface, i.e. at the nodes. These elements resulted the most accurate for this analysis, even if with an increase of computational time;
- the limit contact force normal to the clamps, numerically estimated, is more reliable than the analytical computations based on Hertz theory, because the contact geometry is more detailed and the numerical model accounts for friction;
- an optimal working region was evidenced by the numerical calculations. Working parameters selected within this region allowed the avoidance of any yielding at the wire surface, showing a practical application of the FE model to the drawing machine.

References

Celentano, D.J., Palacios M.A., Rojas E.L., Cruchaga, M.A., Artigas, A.A., 2009. Simulation and experimental validation of multiple-step wire drawing processes. Finite Elements in Analysis and Design 45, 163-180.

Celentano, D.J., 2010. Thermomechanical simulation and experimental validation of wire drawing processes. Materials and Manufacturing Processes 25, 546–556.

Filice, L., Ambrogio, G., Guerriero F., 2013. A multi-objective approach for wire-drawing process. Procedia of the 8th CIRP Conference on Intelligent Computation in Manufacturing Engineering 12, 294-299.

Hertz, H., (1881). On the contact of elastic solids. In: Miscellaneous Papers (MacMillan, London).

Kyo Kabayama, L., Pereira Taguchi, S., Santana Martínez, G.A., 2009. The Influence of Die Geometry on Stress Distribution by Experimental and FEM Simulation on Electrolytic Copper Wiredrawing. Materials Research 12, 3, 281-285.

Sas-Boca, I.M, Tintelecan, M., Pop, M., Ilutiu-Varvara, D-A., Mihu, A.M., 2017. The wire drawing process simulation and the optimization of geometry dies. Procedia Engineering 181, 187-192.

Simulia, Abaqus Manual, v.2017.

Wistreich, J.G., 1958. The Fundamentals of Wire Drawing. Metallurgical Reviews 3, 10, 97–142.

Wriggers, P., 2006. Computational Contact Mechanics. Springer-Verlag, Berlin Heidelberg.

Yang, C.T., 1961 On the mechanics of wire drawing. ASME. Journal of Engineering for Industry 83, 4, 523-529.